Effect of Local Electron-Electron Correlation in Hydrogen-like Impurities in Ge

H. Sims,[1] E. R. Ylvisaker,[2] E. Şaşıoğlu,[3] C. Friedrich,[3] S. Blügel,[3] and W. E. Pickett[2]

[1]*Center for Materials for Information Technology (MINT) and Department of Physics, University of Alabama, Tuscaloosa AL 35487*
[2]*Department of Physics, University of California Davis, Davis CA 95616*
[3]*Peter Grünberg Institut and Institute for Advanced Simulation, Forschungszentrum Jülich and JARA, 52425 Jülich, Germany*

(Dated: February 18, 2013)

We have studied the electronic and local magnetic structure of the hydrogen interstitial impurity at the tetrahedral site in diamond-structure Ge, using an empirical tight binding + dynamical mean field theory approach because within the local density approximation (LDA) Ge has no gap. We first establish that within LDA the 1*s* spectral density bifurcates due to entanglement with the four neighboring sp^3 antibonding orbitals, providing an unanticipated richness of behavior in determining under what conditions a local moment hyperdeep donor or Anderson impurity will result, or on the other hand a gap state might appear. Using a supercell approach, we show that the spectrum, the occupation, and the local moment of the impurity state displays a strong dependence on the strength of the local on-site Coulomb interaction U, the H-Ge hopping amplitude, the depth of the bare 1*s* energy level ϵ_H, and we address to some extent the impurity concentration dependence. In the isolated impurity, strong interaction regime a local moment emerges over most of the parameter ranges indicating magnetic activity, and spectral density structure very near (or in) the gap suggests possible electrical activity in this regime.

I. INTRODUCTION

Due to their importance in electronics technology, isolated defects in semiconductors and insulators have a long history. Low doping levels, arising from isolated shallow defects, provide the carriers that make semiconductors a dominant technology in today's pervasive electronics environment. The primary shallow defects in the more important semiconductors for most applications (Si, GaAs, Ge) have been extensively studied, and research turned to the study of deep levels (states with energies well away from the edges, deep within the gap). An exploration by Haldane and Anderson[1] demonstrated, considering intra-atomic repulsion using the multi-orbital Anderson impurity in a model semiconductor treated in mean field, how multiple charge states can arise and be confined within the semiconducting gap. These charge states will, except accidentally, be deep levels, and when providing a carrier to the conduction band through thermal or electromagnetic excitation, they become deep donor levels.

One of the suspected deep donor impurities in semiconductors, and seemingly the simplest, is interstitial H in an elemental semiconductor. Ge and Si can be prepared ultra-pure, and H possibly is the most common remaining impurity. In work that will be discussed in more detail later, Pickett, Cohen, and Kittel[2] (PCK) provided evidence that interstitial H produces a *hyperdeep donor* level in Ge, with the H 1*s* donor state lying not within the gap but perhaps located as deep as 6 eV *below* the gap, near the center of the valence bands. Their hands-on, self-consistent mean field treatment in the spirit of correlated band theory (LDA+U) methods leaves much yet to be decided.

PCK provided a synopsis of the earlier models that had been applied to this H impurity question. Several H-related defects have been observed[3–7] in Ge, and most seem to be defect complexes in which H is involved, rather than simply isolated H impurities. However, local vibrations were observed for isolated H, identified as (near) bond-centered and in the antibonding or tetrahedral sites,[8,9] which is the impurity of interest here. Similar questions exist for H impurities in the isovalent semiconductors Si [10] and diamond.

Since that early work, a few model studies have addressed the effects of local interactions at a single orbital impurity in a semiconducting host. Yu and Guerrero investigated a one-dimensional Anderson model with an impurity using the density matrix renormalization group approach.[11] The strength of the hybridization compared to the semiconducting gap determined whether the doped-hole density remained localized near the impurity or instead spread over many sites (25 sites in their study). Additional holes were found to be spread throughout the system, avoiding the impurity region. The H in Ge problem is a physical realization of the gapped Anderson impurity model (GAIM) studied by Galpin and Logan.[12,13] They addressed the GAIM with a self-consistent perturbation theory extended to all orders, and concluded that for the half-filled case such as we are in interested in here – neutral H in undoped Ge – for any non-zero gap the interacting system is *not* perturbatively connected to the non-interacting system. This broad claim calls to mind the classic result of Kohn and Majumdar – separate but related, and with different connotations – that the properties of such a system (in the non-interacting case) are *analytic* in the strength of a local potential that drives a bound gap state across the gap edge to become a resonant state in the continuum.[14]

From the earliest electronic structure studies involving H impurities in Ge, most of the focus has been on de-

fect complexes incorporating H with vacancies and other impurities. Model studies[15,16] gave way to a number of density functional theory (DFT) based studies; see Refs. 6 and 7 for representative work. DFT studies of isolated H in Ge and other semiconductors have also been reported,[7,17–19] giving indications that H provides in Ge a shallow donor or shallow acceptor depending on its position (see above), or that it is an example of a negative-U system because of instability of its neutral state. These scenarios, formulated within a quantum theory of energetics (DFT) but a one-electron picture of the spectrum, contrast strikingly with the deep donor possibility posed by PCK. Most of the existing studies confine their focus to energetics of the H-in-Ge system and on "energy level" positions, without an exposition of the spectral distribution of the H 1s weight.

While the H impurity in an elemental semiconductor is the most primitive realization of the impurity problem, this type of system has not seen a material-specific treatment of the dynamical correlations that will influence its electronic structure and excitation spectrum. In this paper we provide results of a dynamical mean field theory (DMFT) treatment[20–22] that sheds light on several of the primary issues.

II. METHOD OF CALCULATION

A. Supercells; host electronic structure

Interstitial H in intrinsic Ge presents a seemingly simple system: a single half-filled 1s orbital hybridized with a semiconducting bath. A neutral H impurity (our interest here) adds one electron that is expected to be accommodated in an additional "state" within the gap or the valence band and most likely the latter, since there has been no signature of an electrically and magnetically active gap state.

Anticipating the disturbance (in density, in screened potential) in an insulator to be localized, we adopt a supercell representation of the impurity. We consider a single interstitial hydrogen atom in the tetrahedrally-symmetric antibonding position in Ge, both in a single (periodic) conventional cubic diamond-structure supercell (containing 8 Ge atoms, denoted HGe_8) and in a $2 \times 2 \times 2$ supercell of conventional cells (containing 64 Ge atoms and denoted HGe_{64}). There is vibrational evidence[8,9] that H sits off the tetrahedral site along a [111] direction, thus closer to one of the four Ge ions than the others, giving it only one Ge nearest neighbor. We do not treat that possibility here, though the methods we use can be applied to that case. Due to a number of uncertainties about materials parameters (and the local density approximation [LDA] gap problem due to the small gap of Ge), we vary the parameters that are not well established, with the goal of obtaining a more general picture of the behavior of a "H-like" interstitial in an elemental tetrahedral semiconductor.

One challenge is to deal with the gap underestimation in LDA. In Ge, the LDA gap is slightly negative, in contrast to the observed gap of 0.8 eV. Since our objective is an initial investigation of dynamical correlations at the H site, we adopt the simplest representation of the Ge electronic structure. Semiconducting Ge will be modeled here using an empirical nearest-neighbor Slater-Koster (S-K) tight-binding model (eTB) consisting of four Wannier orbitals (one s and three p orbitals) per Ge with parameters obtained from the work of Newman and Dow.[23] The H-Ge hopping parameters are taken from the work of Pandey.[24]

B. DMFT parameters

There are, inevitably for the current stage of DMFT theory, two parameters that are not known *a priori*: the Coulomb interaction U and the bare on-site 1s energy ϵ_H with respect to the Ge band gap. For the single orbital problem there is no Hund's rule J_H interaction to be concerned about, nor multiplet effects. In fact, for the isolated H interstitial the DMFT result is exact to within numerical uncertainties. While H-Ge hybridization amplitudes could be extracted from first-principles DFT calculations, since the gap problem in LDA leads us to use an eTB model of the Ge electronic structure, we use eTB hopping amplitudes that were derived in the same spirit.

The hydrogen on-site energy ϵ_H is varied as part of this investigation, guided somewhat by the LDA calculations reported in Sec. III. Within LDA, where there are no parameters, the 1s spectral density for H in the tetrahedral site unexpectedly bifurcates, so there is no clear point of reference for fixing ϵ_H. This splitting is a result of the rather strong hybridization of the 1s orbital with the sp^3 antibonding orbitals of the four surrounding Ge atoms. LDA includes, for a localized state such as a weakly hybridized 1s orbital, a spurious self-interaction that raises the LDA site energy above what is presumed in a LDA+DMFT calculation, providing an extra challenge for determining ϵ_H. The H 1s orbital likely is not a really strongly localized state in Ge, but we expect that ϵ_H = -4 eV should be regarded as upper bound of the bare 1s level. We use the two values -5 eV and -8 eV to span the reasonable range of this parameter. Throughout this paper we use the bottom of the gap at the zero of energy.

The bare (*i.e.* unscreened) on-site repulsion U_0 for an isolated H 1s orbital is $\frac{5}{4}$ Ry = 17.01 eV. This is perhaps surprisingly small for what might seem to be a very small orbital: the 1s orbital of the smallest atom. However, it becomes reasonable once it is recognized that the 1s radial density $4\pi r^2 \rho(r)$ peaks at 1 a_0, whereas the comparable quantity in 3d cations peaks at 0.6-0.9 a_0 and has $U_0 \approx$ 25-30 eV. Screening at a large interstitial site in a small gap insulator is hard to estimate, with no comparable values in the literature. We investi-

gate screened values U=7 eV and U=12 eV to span the likely range. U = 12 eV is not much smaller than the unscreened, isolated H value and should allow the examination of the strong interaction regime. The choice of 7 eV has specific interest: PCK argued[2] that a lone H 1s state would have a bare correlation energy on the order of 1 Ry (our analytic value is actually 17 eV), and that reduction by screening in an insulator would leave a substantial interaction strength of 6–7 eV. This amount of reduction, and more, has over the intervening years become commonplace in understanding the effective values of U in transition metal oxides.

C. Constrained Random-Phase Approximation

Although we vary both parameters in our impurity Hamiltonian (see Sec. II E), as well as the H–Ge hybridization, it is still beneficial to understand the physical value of the interactions in order to both analyze the validity of our range of considered U and of the predictions of PCK and to motivate and guide future material-specific studies. We do this by employing the constrained random-phase approximation (cRPA),[25] performed within the full-potential linearized augmented-plane-wave (FLAPW) method using maximally localized Wannier functions (MLWFs).[26,27] We use the FLAPW method as implemented in the `FLEUR` code[28] with the PBE exchange-correlation potential[29] for the ground-state calculations. MLWFs are constructed with the `Wannier90` code.[30,31] The effective Coulomb potential is calculated within the recently developed cRPA method implemented in the `SPEX` code[32] (for further technical details see Refs. 26, 33, and 34). We use a grid of $6 \times 6 \times 6$ k-points in our HGe_8 cRPA calculations.

The cRPA consists of first writing the polarizability

$$P(\mathbf{r},\mathbf{r}',\omega) = \sum_{\sigma}\sum_{n}^{\text{occ}}\sum_{m}^{\text{unocc}}\left[\frac{\psi^*_{\sigma n}(\mathbf{r})\psi_{\sigma m}(\mathbf{r})\psi^*_{\sigma m}(\mathbf{r}')\psi_{\sigma n}(\mathbf{r}')}{\omega-\varepsilon_{\sigma m}+\varepsilon_{\sigma n}+i\delta} - \frac{\psi_{\sigma n}(\mathbf{r})\psi^*_{\sigma m}(\mathbf{r})\psi_{\sigma m}(\mathbf{r}')\psi^*_{\sigma n}(\mathbf{r}')}{\omega+\varepsilon_{\sigma m}-\varepsilon_{\sigma n}-i\delta}\right], \quad (1)$$

where the ψ_i and ε_i are the DFT wave functions and their eigenvalues, and σ runs over both spin channels. If one separates P into P_l, containing the correlated orbitals, and P_r, containing the rest, and if one considers the unscreened Coulomb operator v, one can write[25,26]

$$U = [1 - vP_r]^{-1}v \quad (2)$$

The matrix elements of the effective Coulomb potential U in the MLWF basis are given by

$$U_{\mathbf{R}n_1n_3;n_4n_2}(\omega) = \iint w^*_{n_1\mathbf{R}}(\mathbf{r})w_{n_3\mathbf{R}}(\mathbf{r})U(\mathbf{r},\mathbf{r}';\omega) \times w^*_{n_4\mathbf{R}}(\mathbf{r}')w_{n_2\mathbf{R}}(\mathbf{r}')\,d^3r\,d^3r', \quad (3)$$

where $w_{n\mathbf{R}}(\mathbf{r})$ is the MLWF at site $\mathbf{R}$ with orbital index n and $U(\mathbf{r},\mathbf{r}';\omega)$ is calculated within the cRPA.

In our calculations, we choose the Ge 4s4p and the H 1s orbitals as our correlated subspace. This is motivated by several considerations. First, we note that, although only the H 1s orbital is treated within DMFT, an interacting picture of the Ge orbitals is necessary to give the correct gapped band structure. In our DMFT calculations, this is accomplished through the eTB Hamiltonian, but here it is necessary to exclude the screening from the Ge sp orbitals in order to get the most accurate picture. The LDA electronic structure (Fig. 1) in Section III A makes clear another reason for the necessity of treating the entire Ge sp + H s subspace within the cRPA: the H 1s state is thoroughly entangled in the Ge 4s and 4p background. In fact, it appears to be split across two bands, frustrating attempts to isolate and manipulate it. Naturally, excluding the Ge sp screening increases the resulting value of the H 1s Hubbard U, which can be considered as an upper limit, and so the value of U most appropriate for our HGe_8 DMFT calculations (in which we only treat the dynamical correlations on the H 1s orbital) is likely smaller than the 11.2 eV we report in Table I. Due to the difference in correlated subspaces considered and the many varied parameters in the DMFT treatment, it is most appropriate to view this cRPA analysis as a separate method for understanding the H impurities and as a way to check the reasonableness of our DMFT approach. We note that the bare (unscreened) value U_b = 16.9 eV is satisfyingly close to the analytic result for U_0 for an isolated H atom (5/4 Ry = 17.0 eV), reflecting the accuracy of the codes.

Orbital	U	J	U_b	J_b
H (1s)	11.2		16.9	
Ge (4s)	7.6		11.9	
Ge (4p)	5.7	0.3	9.2	0.4

TABLE I: cRPA parameters screened Hubbard U and Hund's rule J ($U = F^0 = \frac{1}{(2l+1)^2}\sum_{m,n}U_{mn;mn}$ and $J = \frac{1}{2l(2l+1)}\sum_{m\neq n}U_{mn;nm}$, where l = 0 and 1 for s and p orbitals, respectively) calculated for H 1s and Ge 4s, 4p orbitals in HGe_8, when all sp transitions were excluded. When all transitions are excluded we obtain the bare (unscreened) value U_b and J_b.

	E_s	E_p	$V_{ss\sigma}$	$V_{sp\sigma}$	$V_{pp\sigma}$	$V_{pp\pi}$
Ge	-5.8	1.61	-1.695	-2.03	2.65	-0.67
H–Ge	*	—	-3.30	2.16	—	—

TABLE II: Ge S-K empirical tight-binding parameters (in eV) obtained from Newman and Dow,[23] with H-Ge eTB parameters taken from Pandey.[24] The H s on-site parameter is varied in this study, as are the H-Ge hopping parameters; see the text.

D. Atomic solver

We employ a hybridization-expansion continuous-time (CT-HYB) quantum Monte Carlo impurity solver,[35] taking advantage of the segment picture[36] to simplify the computations. Our solver is based upon that of the ALPS project;[37] we also make use of the ALPS parallel Monte Carlo scheduler.[38] Although the CT-HYB solver has many advantages compared to the interaction-expansion method (CT-INT), the one-electron self energy calculated from CT-HYB is highly sensitive to Monte Carlo noise. The Dyson equation gives the difference between Green's functions obtained from different Monte Carlo simulations, preventing the error from canceling. Indeed, the error in the self-energy is proportional to the absolute error in the Monte Carlo simulation,[39] becoming much larger than the actual data even at relatively low frequencies. Moreover, one cannot accurately determine other quantities that are sensitive to the Green's function and self-energy at all frequencies (such as the occupation of the orbitals). Recently, two complementary solutions to this problem have arisen. Boehnke *et al.*[40] showed that, by measuring the Green's functions in an orthogonal Legendre basis (limited to a relatively small number of polynomials), one can filter out the Monte Carlo noise without losing any accuracy in the computation of the Green's functions and self-energies. Hafermann *et al.*[39] derived an expression for the self-energy involving a quotient of Green's functions rather than a difference. In this formulation, the error in the self-energy is proportional to the relative Monte Carlo error, leading to greatly reduced error into high frequencies. One can combine these methods for further reduction in the error, and we have implemented both.

E. eTB+DMFT Hamiltonian

Our Hamiltonian is that of the Anderson impurity model with a multiorbital "bath," which becomes 256 orbitals for our large cell. It can be represented by the following matrix

$$H^{\mathbf{k}} = \begin{pmatrix} H^{\mathbf{k}}_{\mathrm{Ge}} & V^{\mathbf{k}} \\ \left(V^{\mathbf{k}}\right)^{\dagger} & H_{\mathrm{imp}} \end{pmatrix} \tag{4}$$

where $H^{\mathbf{k}}_{\mathrm{Ge}}$ is the supercell Hamiltonian for Ge obtained from the tight-binding model with no additional interaction parameters included, $V^{\mathbf{k}}$ is the H-Ge hybridization strength, and

$$H_{\mathrm{imp}} = (\epsilon_H - \mu)(\hat{n}_{1s,\uparrow} + \hat{n}_{1s,\downarrow}) + U\hat{n}_{\uparrow}\hat{n}_{\downarrow} \tag{5}$$

is the hydrogen Hamiltonian. There is only a density-density type interaction for a single non-degenerate correlated orbital, as required by the segment formulation of the CT-HYB method. Real frequency spectra are obtained using the maximum entropy (MaxEnt) method[41] as implemented in the ALPS package. Static observables such as the average occupation $\langle n \rangle$, double occupation $\langle n_{\uparrow} n_{\downarrow} \rangle$, and square of the z component of the spin magnetic moment $\langle m_z^2 \rangle$ were measured during the Monte Carlo simulation ($m_z \equiv n_{\uparrow} - n_{\downarrow}$).

III. RESULTS AND DISCUSSION

We present here results relating to a H-like impurity in Ge as a function of the interaction strength U, the magnitude of the H–Ge S-K hopping amplitude, and ϵ_H, at both a 1:8 and a 1:64 H to Ge ratio. We have considered temperatures ranging from $\beta = 5$ eV^{-1} ($T \approx 2300$ K) to $\beta = 40$ eV^{-1} ($T \approx 290$ K). One general observation is that the structure of the spectra that we obtain does not depend very significantly on temperature, so we will neglect temperature dependence in our discussion. In principle, the existence and character of gap states could show significant temperature dependence.

A. LDA and $U = 0$

As presented in the LDA electronic structure of Fig. 1 obtained with the `FPLO` code,[42] the bands with predominantly H 1s character can be readily identified. In both the HGe_8 and HGe_{64} supercells, the H 1s local DOS bifurcates into *two peaks*, one in and just below the gap and the other around -5 eV. Whereas these peaks are effectively separate in the larger cell, they form the boundaries of a broad but bifurcated 1s bandwidth of bandwidth $W \approx 5$–6 eV. The H spectral density is strongly expelled by the hybridization $V^{\mathbf{k}}$ from the large Ge DOS region between these peaks, leaving no clear way to identify an on-site H 1s energy ϵ_H.

The HGe_8 cell result is anomalous in that H appears to introduce *two* new bands (the system is spin-degenerate) in the system, whereas there is but a single 1s orbital. The substantial dispersion of both bands indicates that H interstitials at this concentration are strongly coupled, representing an ordered alloy rather than an isolated impurity. The band structure is in fact metallic, with the upper 1s band partially filled. The occurrence of strong 1s character in two bands is clarified by the results of the HGe_{64} cell: some of the 1s character ($\sim$25%) of the

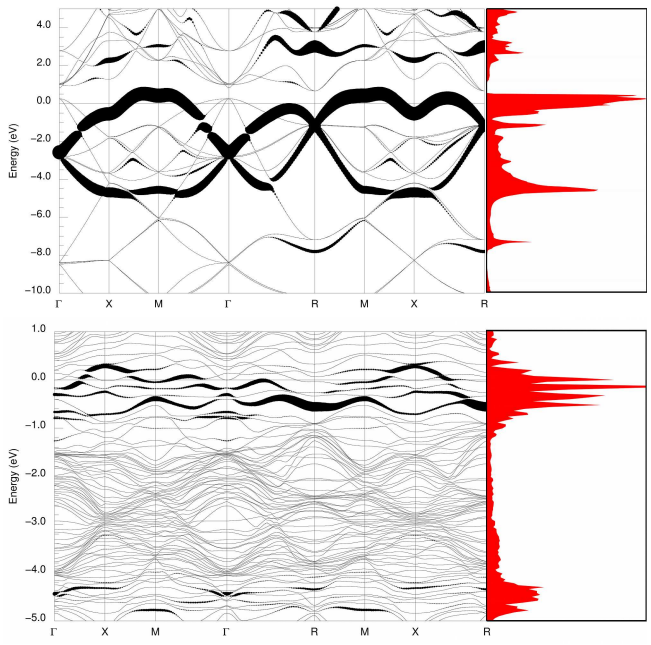

FIG. 1: Left panels: fatbands from LDA emphasizing the H 1s character, indicated by the width of the band. Right panels: H 1s projected density of states from the same calculation. For the HGe_8 cell (top panel) seemingly *two* 1s bands appear, with a total width of nearly 6 eV. The dispersion that is easy to follow reflects H-H interaction within this small cell. In the 64 Ge cell (lower panels), the 1s spectral density is *expelled* from the large Ge DOS region (-4 eV to -1 eV), giving a bifurcation into two peaks separated by 4-5 eV.

character lies 4-5 eV below the gap, with the remained spectral density lying just below the gap and slightly straddling it. The H spectral density within LDA is, as noted above, repelled from the region of large Ge 4p DOS, with part going just below and the majority being pushed near the gap region. This bifurcation of spectral density may account for the fact that correlated band theory (the LDA+U method) was unable to produce a single magnetic hyperdeep state[43] around $\sim$ -5 eV as would be anticipated from the LDA+U method. The HGe_{64} results suggest this large cell is effectively in the isolated impurity limit.

We next survey the non-interacting spectrum (Fig. 2) within our eTB+DMFT picture (using the S-K parameters displayed in Table II). We emphasize that this method is not equivalent to the LDA results just presented; most notably, at full hopping, it contains a gap whereas the LDA bands do not. The gap in fact is larger than the observed value for Ge, but this allows us to assess more confidently the tendency toward formation of a gap state in the type of system we are studying: a H-like interstitial impurity in a Ge-like semiconductor, rather than specifically H in Ge. At reduced H–Ge hybridization the spectrum is dominated by a single Gaussian-like peak centered at ϵ_H, illustrating that the reduced hopping case indeed strongly reduces band structure signatures. At full hopping, the spectrum is substantially spread, with more of the weight appearing above the gap and well below ϵ_H. As anticipated, when ϵ_H is more shallow (-5 eV) the spectral density shows more weight and structure near the gap. Note that, without magnetic order or strong correlation effects (*viz.* in LDA) the Fermi level must fall within the bands, because our supercells contain an odd number of electrons which cannot be insulating with spin degeneracy.

Tables III and IV provide the mean occupancy $\langle n \rangle$, double occupancy $\langle n_\uparrow n_\downarrow \rangle$ and the mean-square moment $\langle m_z^2 \rangle$ (which is also the local susceptibility) for all cases studied. The 1s occupation approaches two electrons in the absence of on-site Coulomb interactions, with the occupation increasing when the impurity level lies deeper and the hybridization is reduced. When $\langle n \rangle > 1$, all Ge states cannot be occupied as just mentioned above, so slight hole-doping will occur leading to a weak acceptor picture. Van de Walle and Neugebauer obtained this type of result[18] in their LDA studies of isolated H in Ge. In the smaller cell, the additional electron density is drawn from all Ge atoms. In the large cell, charge neutrality is accommodated by relatively small re-organization of electron density on the nearby Ge sites.

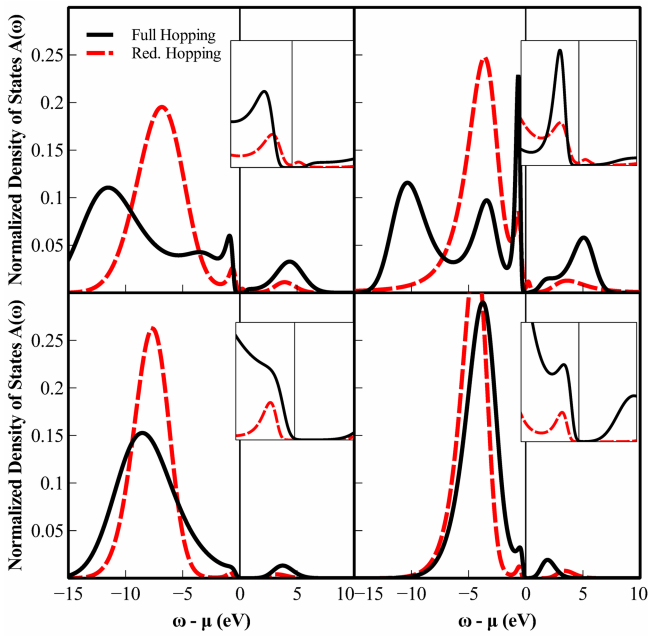

FIG. 2: The H 1s spectral density resulting from eTB+DMFT with $U = 0$, *i.e.* before turning on the interaction. Results are shown for the the two supercells (HGe_8, top panels; HGe_{64}, bottom panels), and for ϵ_H = -8 eV (left panels), and -5 eV (right panels). Reducing the H–Ge hybridization from its full value (full line) leaves a spectrum (dashed line) that is dominated by a Gaussian-like peak centered on ϵ_H. The insets provide an enlargement of the -2 eV to +2 eV regions. In most cases the gap survives (with the exception of the reduced-hopping HGe_8 spectra), providing a test of the MaxEnt procedure.

B. $U = 7$ eV

In the absence of guidance from past work, it seemed reasonable to choose interaction strength U values (reduced from the bare value) that highlight likely points of interest in the relationship between impurity energy level, hybridization strength, and on-site interactions. Choosing $U = 7$ eV probes the behavior when $\epsilon_H + U < 0$ as well as when $\epsilon_H + U > 0$, given our two choices for the $1s$ level. Note that in a mean-field treatment of the interaction, the effective (not bare) H $1s$ level would be at $\epsilon_H + U\langle n\rangle/2$ (since $\langle n_\uparrow\rangle = \langle n_\downarrow\rangle = \langle n\rangle/2$).

Figure 3 shows the spectral functions at $U = 7$ eV, characterized by a large transfer of the spectral weight from ϵ_H at U=0 toward the gap region. The gap clearly survives only in the ϵ_H=-8 eV, large cell case. This dominant effect of U contrasts the modest dependence on the H-Ge hopping strength, though the spectral distribution away from the gap does depend somewhat on V^k. This spectrum shift is accompanied by reduced $1s$ occupation as expected (see Tables III and IV).

At full hybridization strength the H orbital occupation approaches half-filling, particularly when $\epsilon_H = -5$ eV, but double occupation remains substantial, leaving only a small local moment. For reduced hybridization the picture is different. In the ϵ_H=-8 case, a small increase in $1s$ occupation is accompanied by an increase in $\langle m_z^2\rangle$. With a shallower H $1s$ level, however, the orbital remains close to half-filling, and the $1s$ spectra are largely unchanged. Although the structure of the spectrum remains similar, the local moment grows much larger, tending to form a nearly fully-spin-polarized paramagnetic state.

In the HGe_{64} cell, where H-H interaction through the Ge states is negligible, the local moment appears at $\epsilon_H = -5$ at both full and reduced hybridization. In the small cell, the onset of a local moment is accompanied by a large increase in the local DOS near or in the gap brought about by a shift in the sharp low energy peak. However, the large cell shows a reduction or near-vanishing of spectral weight at $\omega - \mu = 0$ irrespective of the magnitude of the local moment.

C. $U = 12$ eV

Increasing the interaction strength to $U = 12$ eV, which is near the cRPA value, prompts some further spreading of the spectral weight and additional sharpening of the spectral peak in the gap region. The $1s$ orbital tends toward half-filling for all parameter values reflecting the strong coupling limit. Qualitatively the spectrum is not affected greatly by the near-doubling of the interaction strength. $\langle m_z^2\rangle$ does increase somewhat for the full value of hybridization. In contrast, reducing the H-Ge hybridization brings about a transition into the local moment state for $\epsilon_H = -8$ eV while leaving the moment on the shallower impurity state about the same as when $U = 7$ eV.

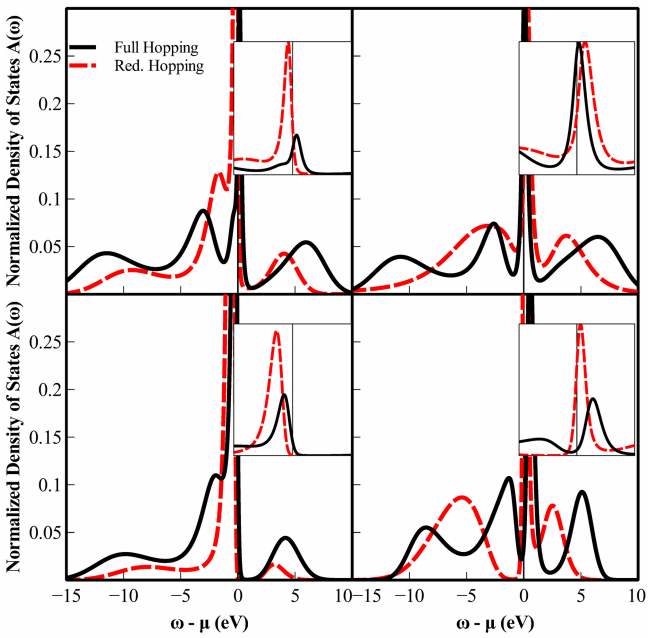

FIG. 3: The introduction of an on-site Coulomb $U = 7$ eV shifts most of the spectral weight to the vicinity of the Ge gap. For $\epsilon_H = -8$ eV (left), two spectral peaks are almost completely occupied, with the higher one overlapping a gap state (actual, or incipient) at 0 eV. The peak is more dramatic near the isolated impurity limit (lower left) and contains almost all of the $1s$ density. The $\epsilon_H = -5$ eV spectra (right) are characterized by a transfer of spectral weight to the Hubbard "bands" (now located on either side of the gap). (inset) A view of the same MaxEnt spectra between -2 and 2 eV.

The $1s$ spectrum of the HGe_{64} cell begins to differ more strongly from that of the smaller cell when the interaction becomes strong. A gap is restored for both values of the H energy level (Fig. 4). Further, the sharp peak now just above the gap begins to dissipate, only just surviving in the $\epsilon_H = -8$ eV spectra at full hopping, while nearly disappearing for reduced hopping in the $\epsilon_H = -5$ spectra. This behavior suggests that a Mott-Hubbard insulating character of the $1s$ spectrum should arise as the impurity limit is approached or as the interaction continues to increase.

D. Transition into the Local Moment State

Transitions to a magnetic local moment state $\langle m_z^2\rangle \sim \mathcal{O}(1)$ occur at different interactions strengths for different values of ϵ_H and H–Ge hopping, and not occurring at all for ϵ_H= -8 eV in the large cell. To shed further light on this transition, we performed a more detailed set of calculations. We varied U between 4 and 12 eV, ϵ_H between -5 and -8 eV, and the H-Ge hopping between 50% and 100% of the eTB value, with all calculations performed in the HGe_8 cell. The results are summarized in Figure 5.

$\mathbf{HGe_8}$		$\epsilon_H = -5$ eV		$\epsilon_H = -8$ eV	
		Full Hopping	Reduced Hopping	Full Hopping	Reduced Hopping
$U = 0$ eV	$\langle n \rangle$	1.66	1.89	1.79	1.94
	$\langle n_\uparrow n_\downarrow \rangle$	0.69	0.89	0.80	0.94
	$\langle m_z^2 \rangle$	0.01	0.00	0.00	0.00
$U = 7$ eV	$\langle n \rangle$	1.04	1.04	1.30	1.60
	$\langle n_\uparrow n_\downarrow \rangle$	0.21	0.12	0.38	0.60
	$\langle m_z^2 \rangle$	**0.07**	**0.58**	**0.04**	**0.10**
$U = 12$ eV	$\langle n \rangle$	0.90	0.99	1.06	1.06
	$\langle n_\uparrow n_\downarrow \rangle$	0.11	0.04	0.18	0.08
	$\langle m_z^2 \rangle$	**0.13**	**0.67**	**0.14**	**0.67**

TABLE III: Local quantities measured during the CT-HYB simulation for the HGe_8 supercell. "Reduced" hopping signifies a tight-binding Hamiltonian in which the H–Ge S-K hopping parameters have been reduced to 50% of the value taken from Ref 24. The double-occupation and local moment show a strong dependence on the magnitude of the H–Ge hopping and the position ϵ_H of the $1s$ level. At half hopping, a large local moment arises for $U = 7$ eV in the shallower state and has nearly saturated by $U = 12$ eV regardless of hopping amplitude. In contrast, the local moment is greatly reduced at all U at full H–Ge hopping.

$\mathbf{HGe_{64}}$		$\epsilon_H = -5$ eV		$\epsilon_H = -8$ eV	
		Full Hopping	Reduced Hopping	Full Hopping	Reduced Hopping
$U = 0$ eV	$\langle n \rangle$	1.94	1.97	1.94	1.74
	$\langle n_\uparrow n_\downarrow \rangle$	0.94	0.97	0.94	0.76
	$\langle m_z^2 \rangle$	0.00	0.00	0.00	0.01
$U = 7$ eV	$\langle n \rangle$	1.08	1.09	1.61	1.80
	$\langle n_\uparrow n_\downarrow \rangle$	0.14	0.10	0.62	0.81
	$\langle m_z^2 \rangle$	0.57	0.80	0.11	0.09
$U = 12$ eV	$\langle n \rangle$	0.99	1.00	1.08	1.02
	$\langle n_\uparrow n_\downarrow \rangle$	0.05	0.01	0.11	0.02
	$\langle m_z^2 \rangle$	0.72	0.94	0.66	0.93

TABLE IV: As in Table III, but for the HGe_{64} supercell. Compared to the smaller cell, the local moment state persists even at full H–Ge hybridization and emerges at smaller values of U.

As indicated in Table III (*i.e.* for the small cell), the paramagnetic local moment is suppressed at full hopping across all U that we consider. The dashed and dotted curves ($\frac{3}{4}$ and $\frac{1}{2}$ hopping, respectively) in Figure 5, however, show much larger moments, with near-complete spin polarization in the H orbital at half hopping. This behavior can be understood both as a direct result of the hybridization and the increase in interaction strength. Within each set of curves, it can be observed that, until relatively large U, the local moment increases with decreasing H level depth. Both this trend and its trend toward reversal at very large U arise from the orbital's proximity to half-filling. Clearly an orbital at half-filling is able to support a larger moment than one well away from half filling. Below $U \approx 8$ eV, only the shallower states are able to push their upper "Hubbard bands" above the gap. At large U, on the other hand, the orbital approaches half-filling regardless of ϵ_H, although for the shallowest $1s$ level, filling falls below unity accompanied by a smaller moment. This tendency to form moments at low effective hybridization and large U is consistent with the infinite-U, HGe_{54} mean-field treatment of PCK, and with lore accumulated in the interim. In addition, this behavior bears some resemblance to that predicted by Li *et al.*[44] for impurities on graphene, where there is a vanishing gap and the environment is two- rather than three-dimensional.

IV. SUMMARY

We have employed dynamical mean field theory using the CT-HYB solver to study the electronic structure of one of the simplest, but still important conceptually and possibly technologically, impurity systems: an interstitial H-like impurity in the antibonding interstitial site in a diamond-structure covalent semiconductor representative of Ge. The non-degenerate $1s$ orbital precludes any

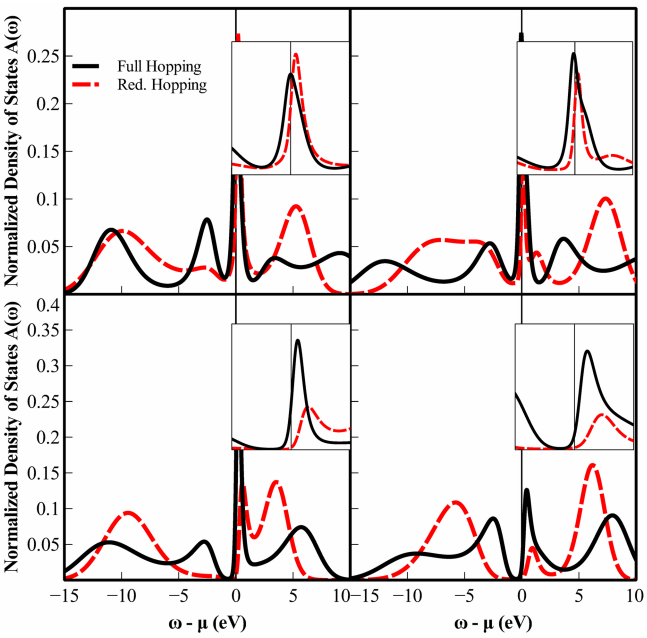

FIG. 4: For strong interactions ($U = 12$ eV), the low-energy quasiparticle-like peak diminishes with respect to the states centered at ϵ_H and in the conduction band. This effect is most dramatic in the 64-Ge cell, where the dominant peak at $U = 7$ is almost completely transferred to higher energy opening or nearly opening a clear gap. In all cases, the 1s orbital approaches half-filling and develops a local moment. (insets) A view of the same MaxEnt spectra between -2 and 2 eV.

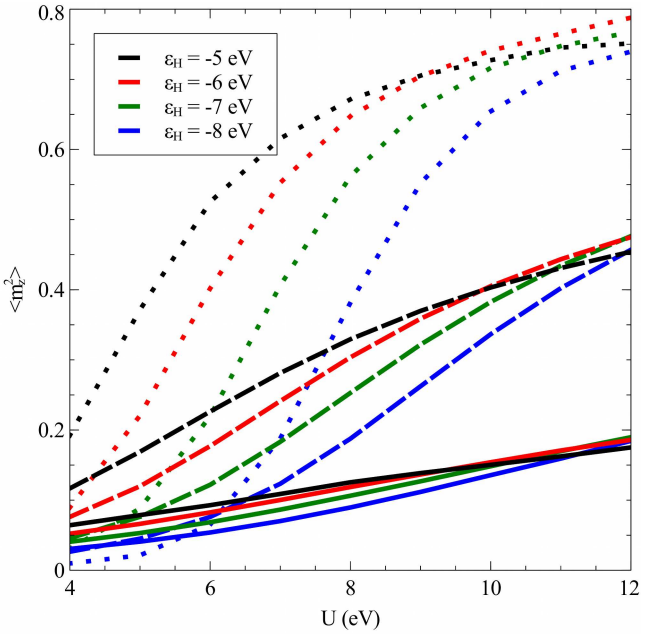

FIG. 5: Monotonic increase of the 1s moment on interaction strength U, for a range of 1s level positions ϵ_H, at full H–Ge hopping amplitude (solid), $\frac{3}{4}$ hopping (dashed), and $\frac{1}{2}$ hopping (dotted). Reduction in H-Ge hybridization results, as expected, in greater spin-polarization in the impurity orbital, but the effect becomes pronounced for reduction below 75% hopping amplitude where the dependence on ϵ_H also becomes strong.

necessity of considering Hund's rule magnetic couping or multiplet effects, so DMFT is the exact solution to the impurity problem in the limit of large supercell. Because Ge within LDA has no gap, the non-interacting system was represented by an empirical tight-binding model with parameters based on previous H-Ge studies.

The H 1s spectrum shows a rich but systematic behavior as the on-site interaction parameter U, the H-Ge hopping amplitude $V^{\mathbf{k}}$, and the H on-site energy ϵ_H are varied, with some parameter ranges possibly giving some insight into Si or diamond hosts as well as Ge. The dependence on temperature was studied but found to be minor, and therefore has not been presented. Our results demonstrate that electron-electron correlations can play a role in determining the properties of the isolated H impurity in such a system. If $\epsilon_H + U/2 > 0$, which naively puts the upper "Hubbard band" above the gap, the on-site Coulomb repulsion is sufficient to prevent the H orbital from acquiring electrons from the surrounding Ge as is the case within LDA.

The behavior of this system is enriched by the bifurcation, at the LDA level, of the 1s spectrum, with much of the weight in and just below the gap and the rest around 4-5 eV binding energy. Within the extended tight-binding model we use and with U=0, which is not exactly the same as within LDA but is closely related, the 1s occupation is 1.7-1.8 reflecting donor character (hole-doping) of Ge before the interaction is turned on. The distributed spectrum primarily through the valence region may be interpreted as the hyper-deep donor character that was envisioned by PCK. Increasing U and/or reducing the hybridization moves the 1s occupation toward unity – Anderson impurity character – with the rate of approach affected by the choice of the bare 1s site energy ϵ_H.

To contribute to a more specific study of H in Ge, we have computed the interaction parameters U and J in HGe_8 for the Ge sp and H s orbitals within the constrained RPA formalism. The H 1s Hubbard U is, as expected, much larger than those associated with the Ge 4s or 4p states, and is coincidentally similar to the largest interaction parameter we considered in our DMFT approach. Further studies are necessary to pin down the behavior of a real H atom in Ge, which will involve optimization of the energy versus H position together with relaxation of the Ge positions. In Si, for example, H more commonly assumes a bond-center position although the tetrahedral interstitial in not far above in energy.[10] The methods needed for those calculations require accurate total energy capability with charge self-consistency, and must include the weak correlation within the Ge sp bands that gets the band gap correct as well as the potentially moderately strong correlation associated with the H im-

purity. As such, this H in Ge problem poses a strong challenge for the future.

V. ACKNOWLEDGMENTS

H.S. wishes to acknowledge helpful conversations with L. Boehnke and H. Hafermann regarding their improved measurement techniques. W.E.P. acknowledges J. C. Smith for discussions of calculations of H interstitials in (insulating) diamond and xenon. Calculations were performed using computational resources from the University of Alabama MINT High Performance Cluster and the NICS Kraken Cray XT5 under XSEDE project TG-PHY120018. W.E.P. acknowledges support from Department of Energy Stewardship Science Academic Alliances program under grant DE-FG03-03NA00071, and E.R.Y. acknowledges support for algorithm development and implementation to the National Science Foundation program Physics at the Information Frontier through grant PHY-1005503. E.Ş, C.F and S.B. acknowledge the support of DFG through the Research Unit FOR-1346.

[1] F. D. M. Haldane and P. W. Anderson, Phys. Rev. B **13**, 2553 (1976).
[2] W. E. Pickett, M. L. Cohen, and C. Kittel, Phys. Rev. B **20**, 5050 (1979).
[3] E. E. Haller, Phys. Rev. Lett. **40**, 584 (1978).
[4] M. Budde, B. Bech Nielsen, R. Jones, J. Goss, and S. Öberg, Phys. Rev. B **54**, 5485 (1996).
[5] J. P. Goss, J. Phys.: Condens. Matter **15**, R551 (2003).
[6] B. J. Coomer, P. Leary, M. Budde, B. Bech Nielsen, R. Jones, S. Öberg, and P. R. Briddon, Matl. Sci. & Eng. B **58**, 36 (1999).
[7] J. Weber, M. Hiller, and E. V. Lavrov, Matl. Sci. Semicond. Processing **9**, 564 (2006).
[8] M. Budde, B. Bech Nielsen, C. P. Cheney, N. H. Tolk, and L. C. Feldman, Phys. Rev. Lett. **85**, 2965 (2000).
[9] C. P. Cheney, M. Budde, G. Lüpke, L. C. Feldman, and N. H. Tolk, Phys. Rev. B **65**, 035214 (2002).
[10] E. A. Davis, J. Non-Crystall. Solids **198-200**, 1 (1996).
[11] C. C. Yu and M. Guerrero, Phys. Rev. B **54**, 8556 (1996).
[12] M. R. Galpin and D. E. Logan, Phys. Rev. B **77**, 195108 (2008).
[13] M. R. Galpin and D. E. Logan, Eur. Phys. J. B **62**, 129 (2008).
[14] W. Kohn and C. Majumdar, Phys. Rev. **138**, A1617 (1965).
[15] J. Oliva and L. M. Falicov, Phys. Rev. B **28**, 7366 (1983).
[16] J. Oliva, Phys. Rev. B **29**, 6846 (1984).
[17] S. K. Estreicher and Dj. M. Maric, Phys. Rev. Lett. **70**, 3963 (1993).
[18] C. G. van de Walle and J. Neugebauer, Nature (London) **423**, 626 (2003).
[19] L. M. Almeida, J. Coutinho, V. J. B. Torres, R. Jones, and P. R. Briddon, Matl. Sci. Semicond. Processing **9**, 503 (2006).
[20] E. Müller-Hartmann, Z. Phys. B **74**, 507 (1989).
[21] W. Metzner and D. Vollhardt, Phys. Rev. Lett. **62**, 324 (1989).
[22] A. Georges and G. Kotliar, Phys. Rev. B **45**, 6479 (1992).
[23] K. E. Newman and J. D. Dow, Phys. Rev. B **30**, 1929 (1984).
[24] K. C. Pandey, Phys. Rev. B **14**, 1557 (1976).
[25] F. Aryasetiawan, M. Imada, A. Georges, G. Kotliar, S. Biermann, and A. I. Lichtenstein, Phys. Rev. B **70**, 195104 (2004); F. Aryasetiawan, K. Karlsson, O. Jepsen, and U. Schönberger, Phys. Rev. B **74**, 125106 (2006); T. Miyake, F. Aryasetiawan, and M. Imada Phys. Rev. B **80**, 155134 (2009); B-C. Shih, Y. Zhang, W. Zhang, and P. Zhang, Phys. Rev. B **85**, 045132 (2012); E. Şaşıoğlu, C. Friedrich, and S. Blügel, Phys. Rev. Lett. **109**, 146401 (2012); H. Sims, W. H. Butler, M. Richter, K. Koepernik, E. Şaşıoğlu, C. Friedrich, and S. Blügel, Phys. Rev. B **86**, 174422 (2012).
[26] E. Şaşıoğlu, C. Friedrich, and S. Blügel, Phys. Rev. B **83**, 121101(R) (2011).
[27] N. Marzari and D. Vanderbilt, Phys. Rev. B **56**, 12847 (1997).
[28] http://www.flapw.de
[29] J. P. Perdew, K. Burke, and M. Ernzerhof, Phys. Rev. Lett. **77**, 3865 (1996).
[30] F. Freimuth, Y. Mokrousov, D. Wortmann, S. Heinze, and S. Blügel, Phys. Rev. B **78**, 035120 (2008).
[31] A. A. Mostofi, J. R. Yates, Y.-S. Lee, I. Souza, D. Vanderbilt, and N. Marzari, Comput. Phys. Commun. **178**, 685 (2008).
[32] C. Friedrich, S. Blügel and A. Schindlmayr, Phys. Rev. B. **81**, 125102 (2010).
[33] E. Şaşıoğlu, A. Schindlmayr, C. Friedrich, F. Freimuth and S. Blügel, Phys. Rev. B. **81**, 054434 (2010).
[34] C. Friedrich, A. Schindlmayr, and S. Blügel, Comp. Phys. Comm. **180**, 347 (2009).
[35] P. Werner and A. J. Millis, Phys. Rev. B **74**, 155107 (2006).
[36] P. Werner, A. Comanac, L. d'Medici, M. Troyer, and A. J. Millis, Phys. Rev. Lett. **97**, 076405 (2006).
[37] E. Gull, P. Werner, S. Fuchs, B. Surer, T. Pruschke, and M. Troyer, Computer Physics Communications **182**, 1078 (2011).
[38] M. Troyer, B. Ammon, and E. Heeb, Lect. Notes Comput. Sci. **1505**, 191 (1998).
[39] H. Hafermann, K. R. Patton, and P. Werner, Phys. Rev. B **85**, 205106 (2012).
[40] L. Boehnke, H. Hafermann, M. Ferrero, F. Lechermann, and O. Parcollet, Phys. Rev. B **84**, 075145 (2011).
[41] R. N. Silver, D. S. Sivia, and J. E. Gubernatis, Phys. Rev. B **41**, 2380 (1990); M. Jarrell and O. Biham, Phys. Rev. Lett. **63**, 2504 (1989).
[42] K. Koepernik and H. Eschrig, Phys. Rev. B **59**, 1743 (1999); http://www.fplo.de
[43] J. C. Smith and W. E. Pickett, unpublished.
[44] C. Li, J.-X. Zhu, and C.S. Ting, arXiv:1106.5827v1.